Dynamic Actuation of Single-Crystal Diamond Nanobeams

Young-Ik Sohn, Michael J. Burek, and Marko Lončar*

School of Engineering and Applied Sciences, Harvard University, 29 Oxford Street, Cambridge, Massachusetts 02138, United States

E-mail: loncar@seas.harvard.edu

KEYWORDS: Single-crystal diamond, nanoelectromechanical systems (NEMS), nanofabrication, dielectrophoresis

Abstract

We show the dielectrophoretic actuation of single-crystal diamond nanomechanical devices using gradient radio-frequency electromagnetic forces. Both cantilever and doubly clamped beams, fabricated using our angled-etching fabrication technique,[1] are demonstrated, with operation frequencies ranging from a few MHz to ∼50 MHz. Frequency tuning and parametric actuation are also studied.

Owing to its large Young' modulus, excellent thermal properties, small thermo-elastic dissipation, *single-crystal* diamond is an ideal candidate for realization of high-frequency (f) and high quality factor (Q) nanoscale mechanical resonators. These devices are of interest for realization of stable, high $f \cdot Q$ product, RF oscillators and inertial sensing applications.[2] Recently, diamond nanomechanical resonators embedded with luminescent crystalline defects (color centers), have also been explored as a promising platform for applications in quantum information science and

*To whom correspondence should be addressed

Report Documentation Page

Form Approved
OMB No. 0704-0188

1. REPORT DATE	2. REPORT TYPE	3. DATES COVERED
25 AUG 2014		**00-00-2014 to 00-00-2014**

4. TITLE AND SUBTITLE	5a. CONTRACT NUMBER
Dynamic Actuation of Single-Crystal Diamond Nanobeams	5b. GRANT NUMBER
	5c. PROGRAM ELEMENT NUMBER
6. AUTHOR(S)	5d. PROJECT NUMBER
	5e. TASK NUMBER
	5f. WORK UNIT NUMBER
7. PERFORMING ORGANIZATION NAME(S) AND ADDRESS(ES) **Harvard University ,School of Engineering and Applied Sciences,Cambridge,MA,02138**	8. PERFORMING ORGANIZATION REPORT NUMBER
9. SPONSORING/MONITORING AGENCY NAME(S) AND ADDRESS(ES)	10. SPONSOR/MONITOR'S ACRONYM(S)
	11. SPONSOR/MONITOR'S REPORT NUMBER(S)

12. DISTRIBUTION/AVAILABILITY STATEMENT
Approved for public release; distribution unlimited

13. SUPPLEMENTARY NOTES

14. ABSTRACT
We show the dielectrophoretic actuation of single-crystal diamond nanomechanical devices using gradient radio-frequency electromagnetic forces. Both cantilever and doubly clamped beams, fabricated using our angled-etching fabrication technique,1 are demonstrated, with operation frequencies ranging from a few MHz to 50 MHz. Frequency tuning and parametric actuation are also studied.

15. SUBJECT TERMS

16. SECURITY CLASSIFICATION OF:			17. LIMITATION OF ABSTRACT	18. NUMBER OF PAGES	19a. NAME OF RESPONSIBLE PERSON
a. REPORT **unclassified**	b. ABSTRACT **unclassified**	c. THIS PAGE **unclassified**	**Same as Report (SAR)**	**19**	

technology (QIST).[3] Of these, negatively charged nitrogen-vacancy (NV^-) color center is of particular interest since it can be used as a spin-qubit with optical read-out. Importantly, NV^- electron spin state can have long coherence times (milliseconds)[4] even at room temperature and it can be prepared and manipulated using microwave and radio frequency (RF) fields to drive transitions between these electron and nuclear spin sublevels.[5–7] Recently, it has been proposed that strain-fields can also be used to manipulate the spin-state of NV,[8,9] which resulted in renewed interest of QIST community in single-crystal diamond micro-electromechanical systems (MEMS).[10–12] For example, coupling between an NV^- center and a mechanical resonator could enable high fidelity control of NV^- spin state via rapid adiabatic passage,[10] and potentially the remote coupling of NV centers via mechanics.[3] Furthermore, mechanical resonators may enable coherent coupling between dissimilar systems with degrees of freedom possessing dramatically different properties and energy scales. To realize such systems, it is essential to achieve a reliable method for controlling and reading the dynamic action of monolithic single-crystal diamond mechanical resonators. To date, only a few reports have demonstrated mechanical resonators fabricated in single-crystal diamond,[13–18] with recent results demonstrating the coupling of NV^- centers to bulk phonon modes[10] and micron-scale mechanical resonators.[11,12] Furthermore, the only true actuator realized in single-crystal diamond relied on heavily boron doped substrates in order to achieve electrostatic actuation for switching applications.[13,14] Such schemes are not easily applied in QIST applications since doping inevitably compromises the diamond material properties and stability of color centers.

Dielectrophoretic actuation[19] has recently been used to actuate and transduce motion of nanoelectromechanical systems (NEMS) and applied to achieve mechanical resonance tuning,[20] and coherent control of classical mechanical resonators,[21] as well as to study cavity electromechanics,[22] and nonlinear mechanics.[23] In our approach, single-crystal diamond cantilevers (Figure 1(a)) and doubly clamped nanobeams (Figure 1(b)) are placed between metal electrodes and are driven by fringing radio-frequency (RF) field (Figure 1(c)) with frequency resonant with mechanical resonance of the devices. Our numerical modeling indicates that keeping small vertical distance from electrodes to nanobeam is of crucial importance for efficient actuation (Figure 1(d)).

In contrast to capacitive and piezo-electric actuation approaches, that may require coating or doping of diamond nanomechanical structure, gradient RF force does not require any modification to the mechanical resonator itself. Therefore, it preserves diamond's unique material properties (Young's modulus, low mass density, large thermal conductivity, and low thermoelastic dissipation) thus minimizing dissipations and resulting in devices with large mechanical quality factors. Of particular interest for QIST applications, dielectrophoretic actuation scheme maintains the integrity and stability of NV centers embedded within diamond nanomechanical structures, that are known to be sensitive to fabrication imperfections and surface terminations.[24] Additionally, we note that electrodes employed for actuation may also double for on-chip delivery of microwave power to NV^- center. Therefore, we believe that dielectrophoretic actuation is an ideal choice for investigation of NV-mechanical coupling.

Our diamond cantilevers and doubly clamped beams are fabricated using fabrication technique–angled-etching–that we have recently developed,[1] which is shown in Figure 2(a). Briefly, angled-etching employs anisotropic oxygen plasma etching at an oblique angle to the substrate surface, yielding suspended triangular cross-section nanobeams directly from single-crystal bulk diamond substrates. Nanomechanical resonators fabricated by angled-etching are easily integrated with dielectrophoretic actuation. The distance from the bottom apex of the suspended nanobeams to the substrate was carefully minimized, since the small vertical distance from on-chip electrodes to the nanobeam is of utmost importance for efficient transduction (Figure 1(c) and (d)). Once free-standing diamond nanobeams were fabricated, electrodes were patterned on the diamond substrate via a standard metal lift-off process. First, the diamond substrate was spin coated with a polymethylmethacrylate-copolymer (MMA/PMMA) bilayer resist, where the MMA copolymer thickness was carefully chosen to be slightly thicker than the distance between the nanobeam top surface and the substrate. Conformal resist coating was observed, without any complication due to existing device geometry. After resist coating, exposure and alignment were done via electron beam lithography. 50 nm of titanium and 200 nm of gold layer were then evaporated and followed by lift-off in remover PG to complete electrode patterning. Figure 2(b) is a top-down view of dia-

mond nanobeam cantilever. It can be seen that good alignment can be achieved, with error on the order of tens of nanometer – this is more than adequate for efficient actuation. In fact, we note that the slight misalignment is actually beneficial since it enables the actuation of in-plane motion, as discussed below. Figure 2(c) shows an array of fabricated diamond doubly clamped nanobeam mechanical resonators that share driving electrodes. This configuration allows us to characterize in parallel large number of resonators having slightly different geometry and hence different resonance frequencies. Our nanomechanical resonators had wide range of widths (200 nm - 300 nm) and lengths (1 μm - 20 μm), corresponding to fundamental flexural resonance frequencies (from Euler-Bernoulli beam theory) ranging from a few MHz to hundreds of MHz. Due to the nature of angled-etching fabrication technique, width and thickness of nanobeam's triangular cross-section are correlated. The smallest cantilever that could be characterized (Figure 1(a)) had a width of 300 nm and the length of 4 μm, while the smallest doubly clamped nanobeam (Figure 1(b)) had a width of 200 nm and the length of 7 μm.

All experiments were performed at room temperature, inside a vacuum chamber at the pressure below 10^{-5} Torr. Figure 3(a) shows a schematic of the experimental setup, which is a slightly modified version of that used previously for characterizing the Brownian motion of single-crystal diamond nanobeams.[17] Specifically, network analyzer was used instead of spectrum analyzer in order to obtain driven response of our devices (by sweeping the driving frequency around mechanical resonance), and a bias-tee was included to combine DC bias with RF drive signal to ensure proper actuation: since actuation force is proportional to the square of applied voltage, $F \propto (V_{DC} + V_{RF} \cos \omega t)^2$.[19] DC bias is needed to provide force component at the driving frequency.

For the most of fabricated diamond nanobeams, both the fundamental out-of-plane and in-plane modes were characterized. Resonant responses of fundamental out-of-plane motion of devices shown in Figure 1(a) and (b) are plotted in Figure 3 (b) and (c), respectively. Solid curves are fitted to the raw data, with both figures showing the expected resonant responses in the linear regime. The maximum resonant frequency of the out-of-plane mode that we could measure using our approach was $\sim$40 MHz, in the case of 7 μm long doubly clamped nanobeam. The maximum

resonant frequency of the in-plane mode, measured in the same devices, was ∼50 MHz. To the best of our knowledge, this is the highest actuation frequency of flexural mechanical vibration achieved by dielectrophoretic actuation to date. Unfortunately, in our current experiments, we were not able to measure devices with resonances >50 MHz, due to the deteriorated signal-to-noise ratio of our measurements. Noise floor of our experiment was affected by three different instruments: shot noise from laser source, dark current and thermal noise from photodetector and thermal noise from the receiver, which can be either the network analyzer or spectrum analyzer. Depending on the settings of instruments, any of these three could be the limiting factor for the noise floor. Most of our measurements, however, were limited by the shot noise from the laser source.

By further increasing the input RF power, and by using longer devices having smaller spring constant, the diamond nanomechanical structures could be driven deep into the nonlinear regime (Figure 4). We note that longer devices are "softer" and therefore deflect more for the same applied voltage, thus easily entering nonlinear regime. Typically, nonlinearity in small scale mechanical resonators can be phenomenologically modeled using Duffing equation:

$$\left[\frac{d^2}{dt^2}+\frac{\Omega_0}{Q}\frac{d}{dt}+\Omega_0^2\left(1+\beta x^2(t)\right)\right]x(t)=\frac{F(t)}{m} \tag{1}$$

where $x(t)$,Ω_0, Q, $F(t)$ and m are the beam displacement, the resonance frequency, mechanical quality factor, external driving force and effective mass of the resonator, respectively. The cubic term $\beta x^3(t)$ in the equation, so called 'Duffing nonlinearity', determines the nonlinear behavior of the resonator: when $\beta < 0$ resonance tends to move to the lower frequency when amplitude increases, resulting in "softening", that is lowering of the spring constant; the opposite is true when $\beta > 0$ and spring "hardening" occurs. Figure 4(a) and (b) shows softening of the fundamental out-of-plane and in-plane modes, respectively, for 8 μm long diamond nanobeam cantilever. On the other hand, spring hardening is observed in the case of 13 μm long doubly clamped diamond nanobeam, for both out-of-plane and in-plane modes shown in Figure 4(c) and (d), respectively.

There are many physical origins that can give rise to mechanical nonlinearities, including, but

are not limited to transduction effects, actuation scheme, material properties, non-ideal boundary conditions, damping mechanics and geometric/inertial effects.[25] Based on our FEM simulations, nonlinearity due to dielectrophoretic actuation can be ruled out due to small deflection (on the order of nanometer) of the resonator. Nonlinearity arising from transduction on nonlinearity can also be ruled out due to the relative small deflection compared to the laser wavelength used. Geometrical nonlinearity is the most common nonlinearity observed in NEMS, and according to theory results in a hardening effect.[26] In contrast, inertial nonlinearity, another physical origin of nonlinearity, always results in a softening behavior.[27] Both of these effects can be significant in our devices, and their interplay determines the overall sign of the Duffing constant and overall softening or hardening.[26]

We characterized two high aspect ratio (length/width > 20) cantilevers and found that they both showed spring softening behavior for their first order out-of-plane and in-plane resonances. Based on these results, we believe that the nonlinear behavior observed in diamond cantilevers is likely due to inertial effects. We also studied ten high aspect-ratio doubly clamped diamond nanobeams, and we observed that the sign of the Duffing constants was not always the same. While in all cases fundamental out-of-plane modes of doubly clamped nanobeams showed spring hardening, the fundamental in-plane modes, however, showed both hardening and softening, without following any particular trend. In fact, even beams of nearly the same geometry on the same chip, revealed opposite mechanical nonlinearites. We believe that theses complexities are caused by residual stress,[17] that was apparent in some high aspect ratio beams that were buckled up or down in post-fabrication SEM images. The sign of the internal stress can cause different types of nonlinearity: for compressive stress spring softening occurs, while for tensile stress spring hardening occurs.[28]

Nonlinear behavior was further confirmed by hysteresis curves as shown in Figure 5(a) and (b), which are measured from fundamental out-of-plane and in-plane modes of 19 μm long doubly clamped diamond nanobeam, respectively. This device was particularly chosen among others as a representative examples because of its prominent nonlinearity, though, other devices gave the hysteresis curves as expected. Further studies, outside the scope of the current manuscript, on

large number of diamond cantilevers are needed, however, to unambiguously identify the physical origin of nonlinearity in diamond cantilevers.

Our dielectrophoretic actuation scheme introduces an additional effective spring since the actuation force has dependence on position.[19] Furthermore, since the force has a quadratic dependence on applied voltage, the mechanical eigenfrequency is tunable with DC bias, and the amount of shift in frequency has quadratic dependence on voltage. Figure 6 (a) shows Brownian motion measured with a spectrum analyzer as the applied DC bias was changed from -9 V to $+9$ V. Bright spots of each data column correspond to the Brownian motion resonance location. The solid black line is a quadratic fit for applied DC bias and shows an excellent match with the theoretical prediction. In the given range of applied DC bias, the mechanical resonance could be tuned over roughly 260 full width at half maximum of the zero bias Brownian motion peak. We observe a blue shift of resonance frequency because this motion is in-plane vibration and the effective spring has always the same sign with the elastic spring. In the case of out-of-plane modes, frequency tuning can be either red or blue shifted, depending on the height of the beam from the driving electrodes.[20]

Since the resonance frequency is easily parametrically tuned more than twice the linewidth, parametric excitation is also expected. Criteria for a resonator to be used for parametric actuation is given in equation (2).[29]

$$\left.\frac{\partial f}{\partial V}\right|_{V_{max}} \cdot V_{max} \cdot \frac{Q}{f_0} > 2 \tag{2}$$

where f, V and Q are resonance frequency, amplitude of applied RF voltage and mechanical quality factor, respectively. f_0 is a resonance frequency without RF voltage input and V_{max} represents the maximum voltage that can be applied. Since the spring constant is a function of position, it can be modeled with Mathieu's equation with a Duffing nonlinearity. Equation (1) may be modified to include parametric tuning as shown below:

$$\left[\frac{d^2}{dt^2} + \frac{\Omega_0}{Q}\frac{d}{dt} + \Omega_0^2\left(1 + \alpha + \beta x^2(t) - 2\Gamma \sin 2\Omega_0 t\right)\right] x(t) = 0 \tag{3}$$

where α is the detuning between the parametric excitation and the fundamental mode Ω_0, Γ

is proportional to the parametric excitation amplitude,[30] whereas other parameters are defined the same way as in equation (1). Right hand side of the equation (3) is zero, since there was no direct driving at resonance frequency. When the resonator with eigenfrequency f_0 can be parametrically excited, its excitation frequency can be $\frac{2f_0}{n}$ for any integer n. In most of the cases, response at $n = 1$ is used since it is the strongest, although the submultiples of it has been observed in experiment.[31] Mathieu's equation with Duffing nonlinearity (3) can be analytically solved and the solution predicts its stability on a phase plane, axes of which are detuning and driving amplitude. Here, we show "instability tongue"[32] when doubly clamped diamond nanobeam is parametrically excited with $n = 1$. In Figure 6 (b) the measured instability tongue is shown when nanobeam was excited around the twice of its natural frequency of 7.25 MHz. In this experiment, excitation was done by RF signal generator and the response was measured with spectrum analyzer, with the amplitude of driven motion was calculated by simple signal processing. Parametric excitation is particularly interesting for NEMS devices since it can circumvent electric cross talk, which can be detrimental for nanoscale system,[33] and can be used to realize a NEMS oscillator[29] and mechanical memory element.[30] Furthermore, parametric oscillators are of interest for mechanical quality factor enhancement,[34] parametric amplification,[35] and noise squeezing.[26]

In summary, we have realized a resonant actuator based on dielectrophoresis for single-crystal diamond nanomechanical systems, thus successfully demonstrating single-crystal diamond NEMS. Actuation of both cantilever and doubly clamped diamond nanobeams was achieved for both the fundamental out-of-plane and in-plane vibrations. Driving frequency range spans from a few MHz to nearly 50 MHz, though higher frequency actuation is expected to be realized by improving the signal-to-noise ratio of the optical interferometric displacement detection, or moving to other low-noise displacement read-out schemes. The dielectrophoretic actuation scheme employed is expected to maintain the mechanical quality factor of the base diamond device, and also to not compromise the optical properties of integrated diamond color centers.

Furthermore, our actuation scheme can efficiently drive the mechanical resonance well into the nonlinear regime, with reasonable RF power levels. Studying physical origins of mechanical non-

linearity in NEMS devices are active field of research, still in its infancy with many open questions unanswered.[36–38] To the best of our knowledge, we believe that our work is the first demonstration of nonlinear mechanical response of single-crystal diamond resonator. Single-crystal diamond has a great potential as a nonlinear NEMS platform due to its ultrahigh mechanical quality factor. Recently, it has been shown that single-crystal diamond resonators can have mechanical quality factor over 300,000[18] or even over a million[16] at room temperature. In this regard, the capability of our system to preserve high mechanical quality factor is of great importance in the study and application of nonlinear mechanics. Although pre-stressed nitrides in general show the highest quality factor in NEMS,[38] it is not suitable to study nonlinear mechanics because of its strong tensile stress.[26]

Lastly, our actuation scheme is capable of strong frequency tuning simply by applying DC bias, and leads to useful parametric excitation. Parametric excitation is expected to be important in many applications including NV^- center engineering, since actuation signals can be completely filtered out from desired NV^- center manipulation/read-out signals in frequency domain. Single-crystal diamond actuation we developed here is expected to be a gateway to a more sophisticated platform for the control of NV^- center via nanoscale mechanics.

Acknowledgement

This work was performed in part at the Center for Nanoscale Systems (CNS), a member of the National Nanotechnology Infrastructure Network (NNIN), which is supported by the National Science Foundation under NSF award no. ECS-0335765. CNS is part of Harvard University. Authors acknowledge the financial support from STC Center for Integrated Quantum Materials (NSF grant DMR-1231319), the Defense Advanced Research Projects Agency (QuASAR program), and AFOSR MURI (grant FA9550-12-1-0025). M.J. Burek is supported in part by the Natural Science and Engineering Council (NSERC) of Canada.

References

(1) Burek, M. J.; de Leon, N. P.; Shields, B. J.; Hausmann, B. J. M.; Chu, Y.; Quan, Q.; Zibrov, A. S.; Park, H.; Lukin, M. D.; Lončar, M. *Nano Letters* **2012**, *12*, 6084–6089.

(2) Kusterer, J.; Kohn, E. *CVD Diamond MEMS*; Wiley Online Library, 2009; pp 467–544.

(3) Rabl, P.; Kolkowitz, S. J.; Koppens, F. H. L.; Harris, J. G. E.; Zoller, P.; Lukin, M. D. *Nature Physics* **2010**, *6*, 602–608.

(4) Balasubramanian, G.; Neumann, P.; Twitchen, D.; Markham, M.; Kolesov, R.; Mizuochi, N.; Isoya, J.; Achard, J.; Beck, J.; Tissler, J.; Jacques, V.; Hemmer, P. R.; Jelezko, F.; Wrachtrup, J. *Nature Materials* **2009**, *8*, 383–387.

(5) van der Sar, T.; Wang, Z. H.; Blok, M. S.; Bernien, H.; Taminiau, T. H.; Toyli, D. M.; Lidar, D. A.; Awschalom, D. D.; Hanson, R.; Dobrovitski, V. V. *Nature* **2012**, *484*, 82–86.

(6) Jiang, L.; Hodges, J. S.; Maze, J. R.; Maurer, P.; Taylor, J. M.; Cory, D. G.; Hemmer, P. R.; Walsworth, R. L.; Yacoby, A.; Zibrov, A. S.; Lukin, M. D. *Science* **2009**, *326*, 267–272.

(7) Dutt, M. V. G.; Childress, L.; Jiang, L.; Togan, E.; Maze, J.; Jelezko, F.; Zibrov, A. S.; Hemmer, P. R.; Lukin, M. D. *Science* **2007**, *316*, 1312–1316.

(8) Bennett, S. D.; Yao, N. Y.; Otterbach, J.; Zoller, P.; Rabl, P.; Lukin, M. D. *Physical Review Letters* **2013**, *110*, 156402.

(9) Kepesidis, K. V.; Bennett, S. D.; Portolan, S.; Lukin, M. D.; Rabl, P. *Physical Review B* **2013**, *88*, 064105.

(10) MacQuarrie, E. R.; Gosavi, T. A.; Jungwirth, N. R.; Bhave, S. A.; Fuchs, G. D. *Physical Review Letters* **2013**, *111*, 227602.

(11) Ovartchaiyapong, P.; Lee, K. W.; Myers, B. A.; Jayich, A. C. B. *arXiv.org* **2014**,

(12) Teissier, J.; Barfuss, A.; Appel, P.; Neu, E.; Maletinsky, P. *ArXiv e-prints* **2014**,

(13) Liao, M.; Rong, Z.; Hishita, S.; Imura, M.; Koizumi, S.; Koide, Y. *Diamond & Related Materials* **2012**, *24*, 69–73.

(14) Liao, M.; Hishita, S.; Watanabe, E.; Koizumi, S.; Koide, Y. *Advanced Materials* **2010**, *22*, 5393–5397.

(15) Zalalutdinov, M. K.; Ray, M. P.; Photiadis, D. M.; Robinson, J. T.; Baldwin, J. W.; Butler, J. E.; Feygelson, T. I.; Pate, B. B.; Houston, B. H. *Nano Letters* **2011**, *11*, 4304–4308.

(16) Tao, Y.; Boss, J. M.; Moores, B. A.; Degen, C. L. *Nature Communications* **2014**, *5*, 1–8.

(17) Burek, M. J.; Ramos, D.; Patel, P.; Frank, I. W.; Lončar, M. *Applied Physics Letters* **2013**, *103*, 131904–131904–5.

(18) Ovartchaiyapong, P.; Pascal, L. M. A.; Myers, B. A.; Lauria, P.; Bleszynski Jayich, A. C. *Applied Physics Letters* **2012**, *101*, 163505.

(19) Unterreithmeier, Q. P.; Weig, E. M.; Kotthaus, J. P. *Nature* **2009**, *458*, 1001–1004.

(20) Rieger, J.; Faust, T.; Seitner, M. J.; Kotthaus, J. P.; Weig, E. M. *Applied Physics Letters* **2012**, *101*, 103110.

(21) Faust, T.; Rieger, J.; Seitner, M. J.; Kotthaus, J. P.; Weig, E. M. *Nature Physics* **2013**, *9*, 485–488.

(22) Faust, T.; Krenn, P.; Manus, S.; Kotthaus, J. P.; Weig, E. M. *Nature Communications* **2012**, *3*, 728–.

(23) Unterreithmeier, Q. P.; Faust, T.; Kotthaus, J. P. *Physical Review B* **2010**, *81*, 241405.

(24) Chu, Y.; de Leon, N. P.; Shields, B. J.; Hausmann, B. *Nano . . .* **2014**,

(25) Villanueva, L. G.; Karabalin, R. B.; Matheny, M. H.; Chi, D.; Sader, J. E.; Roukes, M. L. *Phys. Rev. B* **2013**, *87*, 024304.

(26) Lifshitz, R.; Cross, M. *Reviews of nonlinear dynamics and complexity* **2008**, *1*, 1–48.

(27) Villanueva, L. G.; Karabalin, R. B.; Matheny, M. H.; Chi, D.; Sader, J. E.; Roukes, M. L. *Physical Review B* **2013**, *87*, 024304.

(28) Rath, P.; Khasminskaya, S.; Nebel, C.; Wild, C.; Pernice, W. H. P. *Nat Commun* **2013**, *4*, 1690.

(29) Villanueva, L. G.; Karabalin, R. B.; Matheny, M. H.; Kenig, E.; Cross, M. C.; Roukes, M. L. *Nano Letters* **2011**, *11*, 5054–5059.

(30) Mahboob, I.; Yamaguchi, H. *Nature nanotechnology* **2008**, *3*, 275–279.

(31) Turner, K. L.; Miller, S. A.; Hartwell, P. G.; MacDonald, N. C.; Strogatz, S. H.; Adams, S. G. *Nature* **1998**, *396*, 149–152.

(32) Nayfeh, A. H.; Mook, D. T. *Nonlinear Oscillations*; John Wiley & Sons, 2008.

(33) Feng, X. L.; White, C. J.; Hajimiri, A.; Roukes, M. L. *Nature nanotechnology* **2008**, *3*, 342–346.

(34) Mahboob, I.; Yamaguchi, H. *Applied Physics Letters* **2008**, *92*, 253109.

(35) Suh, J.; LaHaye, M. D.; Echternach, P. M.; Schwab, K. C.; Roukes, M. L. *Nano Letters* **2010**, *10*, 3990–3994.

(36) Kacem, N.; Hentz, S.; Pinto, D.; Reig, B.; Nguyen, V. *Nanotechnology* **2009**, *20*, 275501.

(37) Kacem, N.; Arcamone, J.; Perez-Murano, F.; Hentz, S. *Control of buckling in large micromembranes using engineered support structures* **2010**, *20*, 045023.

(38) Imboden, M.; Williams, O.; Mohanty, P. *Applied Physics Letters* **2013**, *102*, 103502.

styleapsrev

References

(1) Burek, M. J.; de Leon, N. P.; Shields, B. J.; Hausmann, B. J. M.; Chu, Y.; Quan, Q.; Zibrov, A. S.; Park, H.; Lukin, M. D.; Lončar, M. *Nano Letters* **2012**, *12*, 6084–6089.

(2) Kusterer, J.; Kohn, E. *CVD Diamond MEMS*; Wiley Online Library, 2009; pp 467–544.

(3) Rabl, P.; Kolkowitz, S. J.; Koppens, F. H. L.; Harris, J. G. E.; Zoller, P.; Lukin, M. D. *Nature Physics* **2010**, *6*, 602–608.

(4) Balasubramanian, G.; Neumann, P.; Twitchen, D.; Markham, M.; Kolesov, R.; Mizuochi, N.; Isoya, J.; Achard, J.; Beck, J.; Tissler, J.; Jacques, V.; Hemmer, P. R.; Jelezko, F.; Wrachtrup, J. *Nature Materials* **2009**, *8*, 383–387.

(5) van der Sar, T.; Wang, Z. H.; Blok, M. S.; Bernien, H.; Taminiau, T. H.; Toyli, D. M.; Lidar, D. A.; Awschalom, D. D.; Hanson, R.; Dobrovitski, V. V. *Nature* **2012**, *484*, 82–86.

(6) Jiang, L.; Hodges, J. S.; Maze, J. R.; Maurer, P.; Taylor, J. M.; Cory, D. G.; Hemmer, P. R.; Walsworth, R. L.; Yacoby, A.; Zibrov, A. S.; Lukin, M. D. *Science* **2009**, *326*, 267–272.

(7) Dutt, M. V. G.; Childress, L.; Jiang, L.; Togan, E.; Maze, J.; Jelezko, F.; Zibrov, A. S.; Hemmer, P. R.; Lukin, M. D. *Science* **2007**, *316*, 1312–1316.

(8) Bennett, S. D.; Yao, N. Y.; Otterbach, J.; Zoller, P.; Rabl, P.; Lukin, M. D. *Physical Review Letters* **2013**, *110*, 156402.

(9) Kepesidis, K. V.; Bennett, S. D.; Portolan, S.; Lukin, M. D.; Rabl, P. *Physical Review B* **2013**, *88*, 064105.

(10) MacQuarrie, E. R.; Gosavi, T. A.; Jungwirth, N. R.; Bhave, S. A.; Fuchs, G. D. *Physical Review Letters* **2013**, *111*, 227602.

(11) Ovartchaiyapong, P.; Lee, K. W.; Myers, B. A.; Jayich, A. C. B. *arXiv.org* **2014**,

(12) Teissier, J.; Barfuss, A.; Appel, P.; Neu, E.; Maletinsky, P. *ArXiv e-prints* **2014**,

(13) Liao, M.; Rong, Z.; Hishita, S.; Imura, M.; Koizumi, S.; Koide, Y. *Diamond & Related Materials* **2012**, *24*, 69–73.

(14) Liao, M.; Hishita, S.; Watanabe, E.; Koizumi, S.; Koide, Y. *Advanced Materials* **2010**, *22*, 5393–5397.

(15) Zalalutdinov, M. K.; Ray, M. P.; Photiadis, D. M.; Robinson, J. T.; Baldwin, J. W.; Butler, J. E.; Feygelson, T. I.; Pate, B. B.; Houston, B. H. *Nano Letters* **2011**, *11*, 4304–4308.

(16) Tao, Y.; Boss, J. M.; Moores, B. A.; Degen, C. L. *Nature Communications* **2014**, *5*, 1–8.

(17) Burek, M. J.; Ramos, D.; Patel, P.; Frank, I. W.; Lončar, M. *Applied Physics Letters* **2013**, *103*, 131904–131904–5.

(18) Ovartchaiyapong, P.; Pascal, L. M. A.; Myers, B. A.; Lauria, P.; Bleszynski Jayich, A. C. *Applied Physics Letters* **2012**, *101*, 163505.

(19) Unterreithmeier, Q. P.; Weig, E. M.; Kotthaus, J. P. *Nature* **2009**, *458*, 1001–1004.

(20) Rieger, J.; Faust, T.; Seitner, M. J.; Kotthaus, J. P.; Weig, E. M. *Applied Physics Letters* **2012**, *101*, 103110.

(21) Faust, T.; Rieger, J.; Seitner, M. J.; Kotthaus, J. P.; Weig, E. M. *Nature Physics* **2013**, *9*, 485–488.

(22) Faust, T.; Krenn, P.; Manus, S.; Kotthaus, J. P.; Weig, E. M. *Nature Communications* **2012**, *3*, 728–.

(23) Unterreithmeier, Q. P.; Faust, T.; Kotthaus, J. P. *Physical Review B* **2010**, *81*, 241405.

(24) Chu, Y.; de Leon, N. P.; Shields, B. J.; Hausmann, B. *Nano . . .* **2014**,

(25) Villanueva, L. G.; Karabalin, R. B.; Matheny, M. H.; Chi, D.; Sader, J. E.; Roukes, M. L. *Phys. Rev. B* **2013**, *87*, 024304.

(26) Lifshitz, R.; Cross, M. *Reviews of nonlinear dynamics and complexity* **2008**, *1*, 1–48.

(27) Villanueva, L. G.; Karabalin, R. B.; Matheny, M. H.; Chi, D.; Sader, J. E.; Roukes, M. L. *Physical Review B* **2013**, *87*, 024304.

(28) Rath, P.; Khasminskaya, S.; Nebel, C.; Wild, C.; Pernice, W. H. P. *Nat Commun* **2013**, *4*, 1690.

(29) Villanueva, L. G.; Karabalin, R. B.; Matheny, M. H.; Kenig, E.; Cross, M. C.; Roukes, M. L. *Nano Letters* **2011**, *11*, 5054–5059.

(30) Mahboob, I.; Yamaguchi, H. *Nature nanotechnology* **2008**, *3*, 275–279.

(31) Turner, K. L.; Miller, S. A.; Hartwell, P. G.; MacDonald, N. C.; Strogatz, S. H.; Adams, S. G. *Nature* **1998**, *396*, 149–152.

(32) Nayfeh, A. H.; Mook, D. T. *Nonlinear Oscillations*; John Wiley & Sons, 2008.

(33) Feng, X. L.; White, C. J.; Hajimiri, A.; Roukes, M. L. *Nature nanotechnology* **2008**, *3*, 342–346.

(34) Mahboob, I.; Yamaguchi, H. *Applied Physics Letters* **2008**, *92*, 253109.

(35) Suh, J.; LaHaye, M. D.; Echternach, P. M.; Schwab, K. C.; Roukes, M. L. *Nano Letters* **2010**, *10*, 3990–3994.

(36) Kacem, N.; Hentz, S.; Pinto, D.; Reig, B.; Nguyen, V. *Nanotechnology* **2009**, *20*, 275501.

(37) Kacem, N.; Arcamone, J.; Perez-Murano, F.; Hentz, S. *Control of buckling in large micromembranes using engineered support structures* **2010**, *20*, 045023.

(38) Imboden, M.; Williams, O.; Mohanty, P. *Applied Physics Letters* **2013**, *102*, 103502.

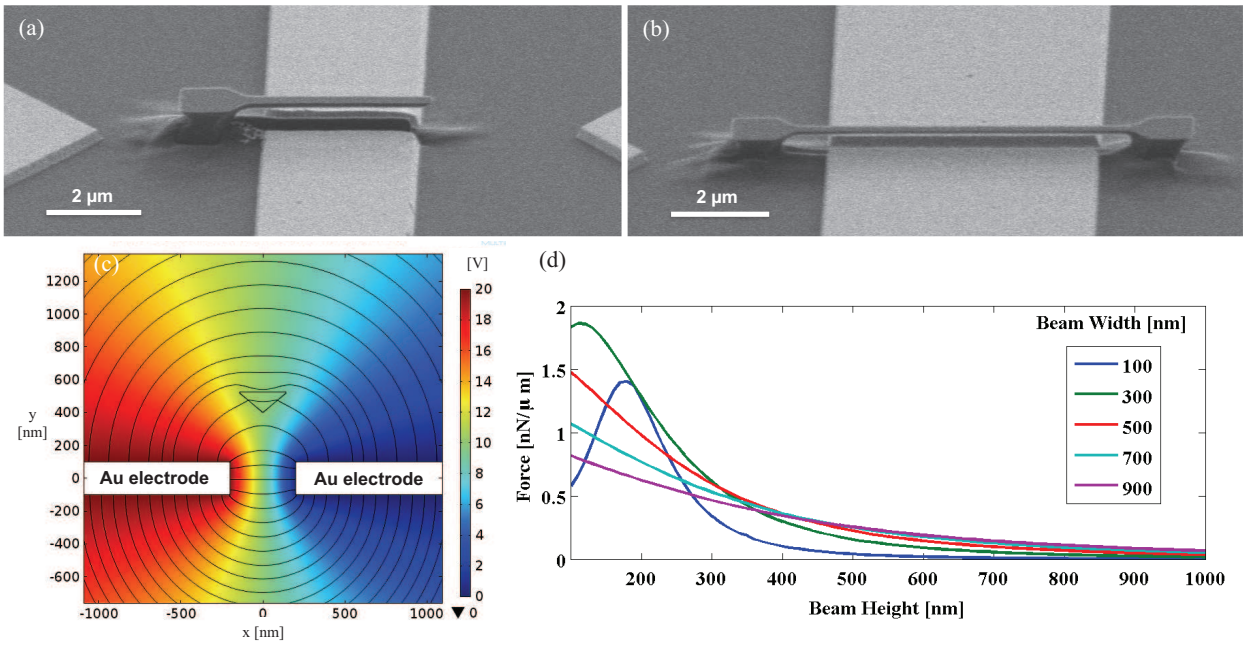

Figure 1: SEM images of (a) 4 μm cantilever and (b) 7 μm doubly clamped beam. These represent the shortest devices that could be characterized to date. (c) Finite element method (FEM) simulation is used to calculate applied force to suspended nanobeam with a given geometry and electrostatic environment. Color map stands for the voltage and the streamlines show corresponding electric field. (d) Vertical force per unit length applied to the beam from (c) is plotted as a function of beam width and height, in which applied voltage of 20 V was assumed. It can be seen that force is maximized when height is small. In fact, there is an optimal position that mazimizes the force, since force goes to zero in the middle of two electrodes due to the symmetry and it also goes to zero at the far distance due to the lack of electrical field gradient.

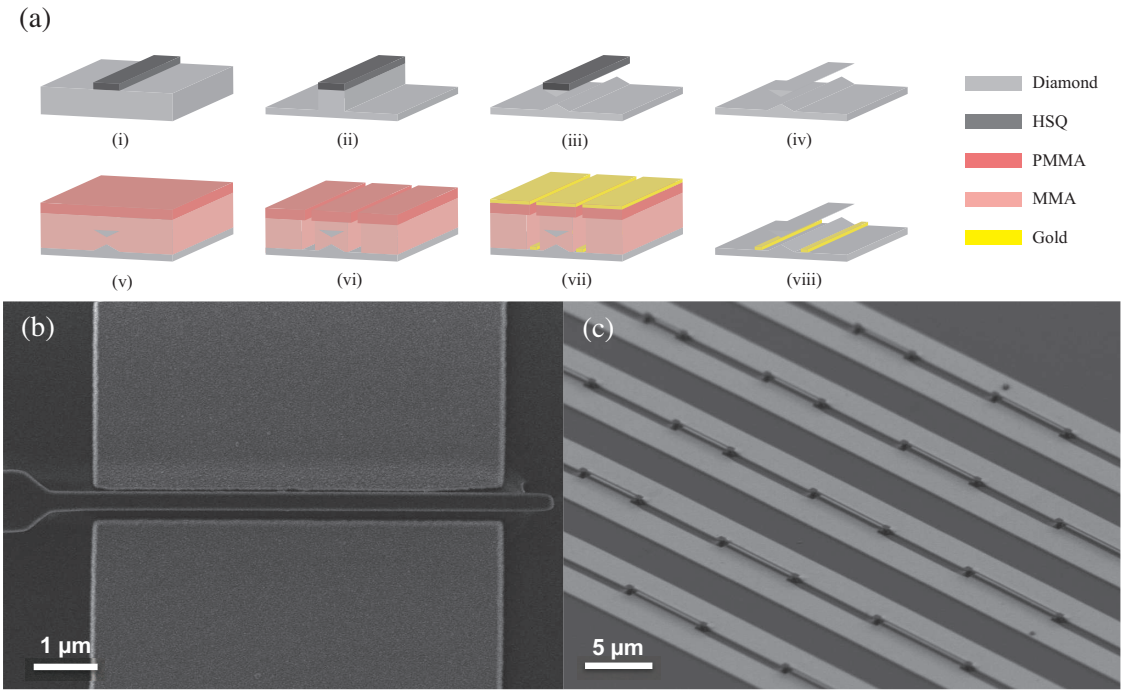

Figure 2: (a) Schematic illustration of angled-etching nanofabrication of for suspended diamond nanobeams and the following standard bi-layer MMA/PMMA process for lift-off. Each step is composed as the following: (i) Electron beam lithography mask is deposited, (ii) top-down reactive ion etching of diamond is performed, followed by the (iii) angled-etching step and (iv) mask removal. (v) New e-beam resist is deposited, and (vi) electron beam lithography followed by (vii) metal evaporation and (viii) lift-off are used to define electrodes. (b) High mag SEM image of 7 μm cantilever shows that good alignment can be achieved, on the order of tens of nanometers, which allows for efficient actuation. (c) SEM image of device array sharing electrodes.

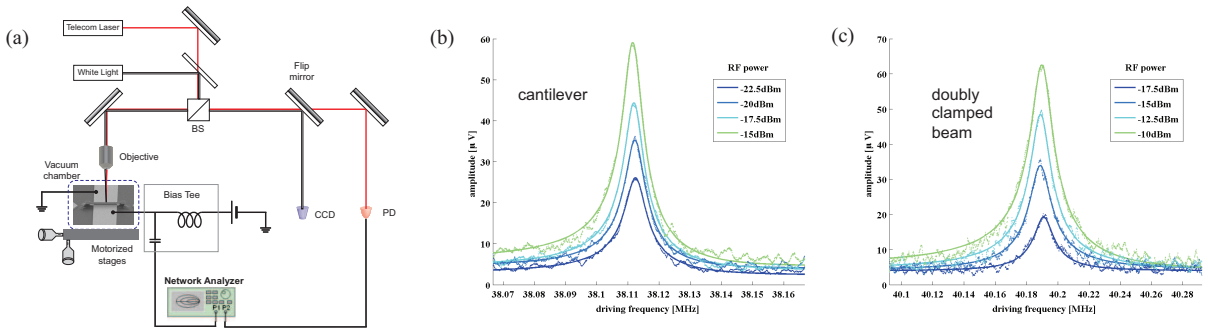

Figure 3: (a) Optical characterization setup. Fundamental out-of-plane resonant response of devices shown in Figure 1(a) and (b) are given in (b) and (c), respectively.

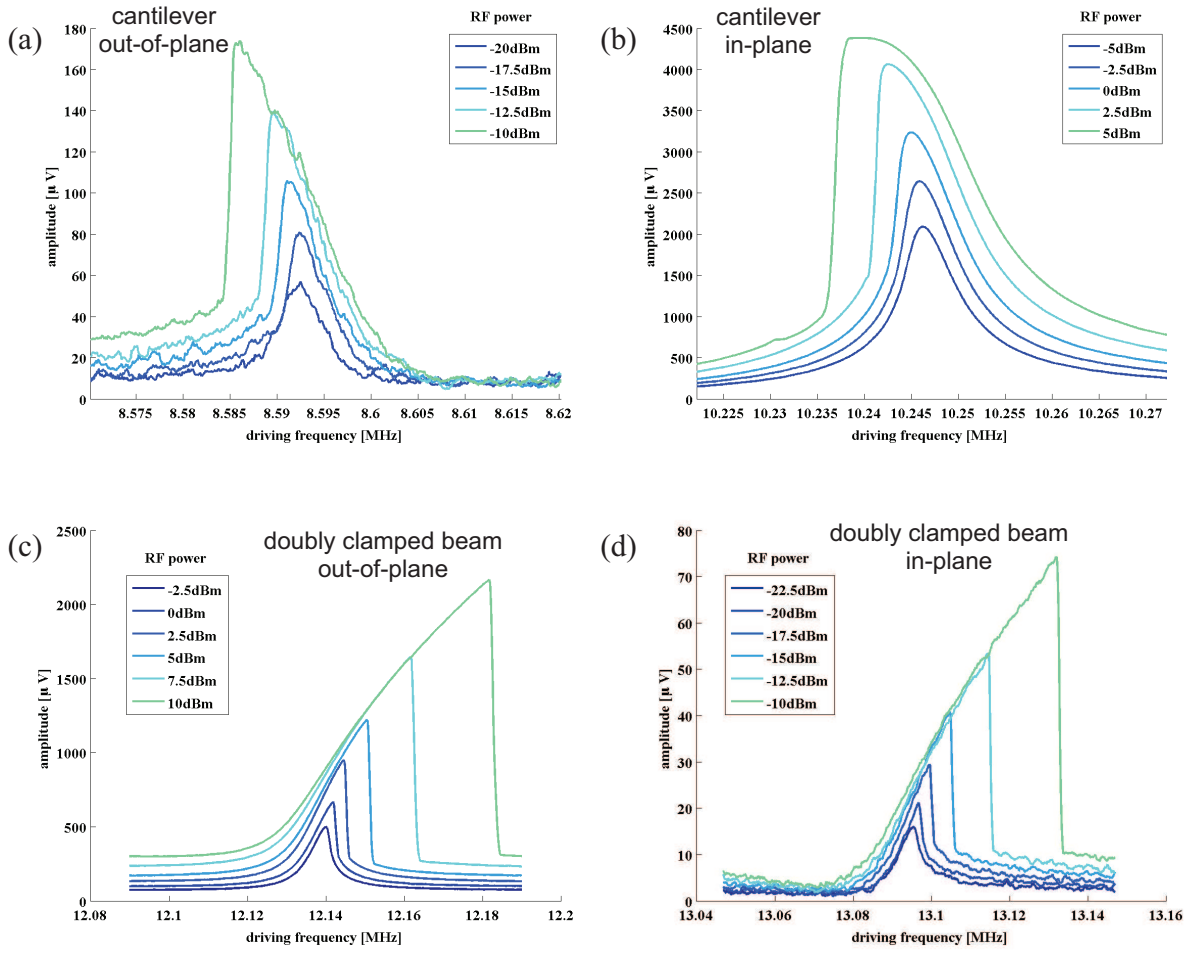

Figure 4: When nanobeams are driven hard enough, they start to show nonlinear behavior. Nonlinear response of 8 μm long cantilever for its (a) out-of-plane and (b) in-plane modes. Softening of spring was observed for both types of modes. On the other hand, spring hardening was observed in the case of strongly driven 13 μm long doubly clamped diamond nanobeam both for its (c) out-of-plane and (d) in-plane modes.

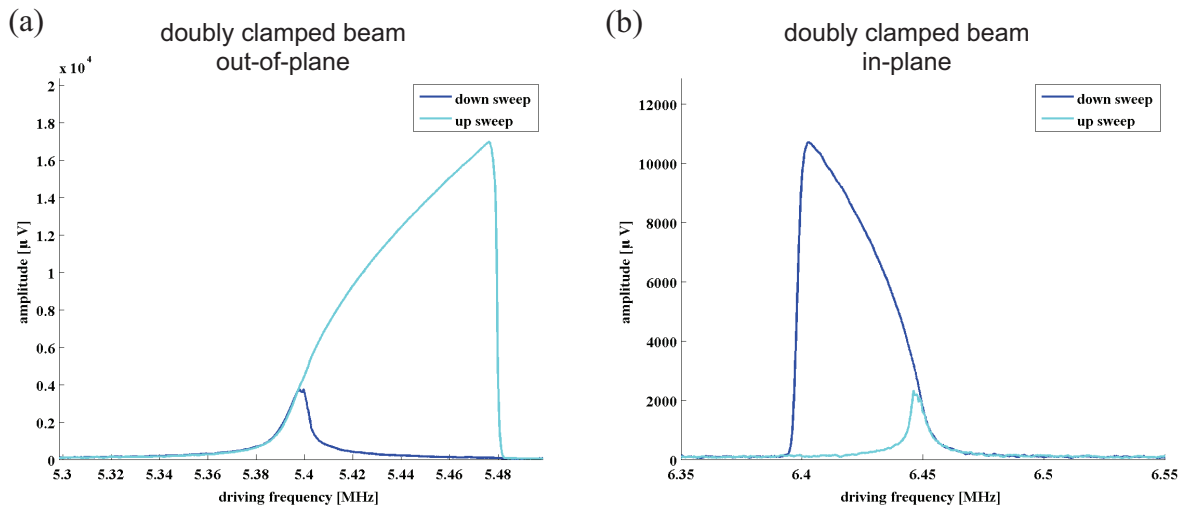

Figure 5: Hysteresis curve of (a) hardening and (b) softening mechanical nonlinearity measured from 19 μm long doubly clamped diamond nanobeam when frequency was swept up and down. (a) and (b) are the fundamental out-of-plane and in-plane modes, respectively.

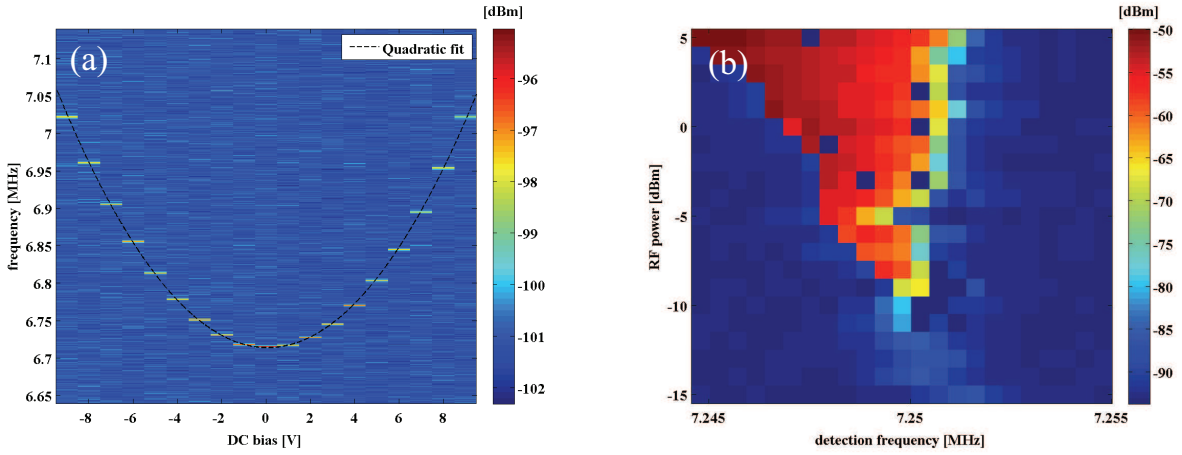

Figure 6: (a) Tuning of mechanical resonance using DC bias. With applying $\pm$9V, frequency tuning range that can be achieved is approximately 260 linewidths. Quadratic nature of tuning can be used to control the onset of parametric instability in terms of RF power. (b) Typical tongue shape of parametric instability was observed. Low response spots inside the instability region are attributed to data acquisition software problems.